

Investigations on LED illumination for micro-PIV including a novel front-lit configuration

S. M. Hagsäter · C. H. Westergaard ·
H. Bruus · J. P. Kutter

Received: 30 March 2007 / Revised: 6 September 2007 / Accepted: 6 September 2007 / Published online: 11 October 2007
© Springer-Verlag 2007

Abstract In this study, we provide a general investigation on micro-PIV with LED illumination. A number of improvements over previous LED-based systems are suggested, in particular, we present a novel front-lit configuration. As a demonstration of its versatility we have used this front-lit configuration to perform micro-PIV measurements around a 50 μm squared pillar in a micro-channel with rectangular cross section, in both fluorescent mode and scattered mode. A comparison between the two modes is supplied, showing very good agreement between the respective velocity field results.

1 Introduction

Micro-PIV is a technique developed for measuring flow fields in microfluidic systems (Santiago et al. 1998). In a typical particle image velocimetry (PIV) experiment, a light sheet formed by a laser is used to illuminate only a section of the flow, where the thickness of the light sheet is smaller than the depth of focus of the image recording

system. In most cases, this approach is impractical for micro-PIV, and instead so-called volume illumination is applied (Meinhart et al. 2000a). Here, the whole volume of the flow is illuminated, and now the depth of focus of the microscope objective defines the measurement region.

Dual cavity lasers, capable of delivering more than 10 mJ at pulse lengths typically in the range of 10–100 ns, originally developed for PIV, are also excellent for use in micro-PIV. However, for most microfluidic investigations the full capacity of these lasers is not utilized. Continuous light sources, such as arc lamps or CW-lasers, can also be used for volume illumination. Their applicability is highly dependant on the type of recording camera, but without the use of a shutter they are generally limited to low velocity flows.

In this article, we will show that light emitting diodes (LEDs) are well suited for micro-PIV, and a new, more versatile illumination configuration will be introduced. PIV with LED illumination is little described in the literature. Estevadeordal and Goss (2005) have demonstrated LED illumination PIV with shadows of particles in air-flow. They also demonstrated measurements in pulse mode and supplied a discussion on some general considerations for PIV with LEDs. Chételat and Kim (2002) presented a MPIV (miniature PIV) system with LED illumination, also including a discussion on alternative illumination variants.

Since the experimental conditions in micro-PIV are considerably different to those in larger scale PIV, a separate investigation and description of LED illumination for micro-PIV is appropriate. There are a few previous micro-PIV studies where LEDs have been used as illumination sources, for example in the work of Singh et al. (2001) and Bitsch et al. (2005). However, these articles did not consider specific aspects of the LED illumination configurations.

S. M. Hagsäter (✉) · H. Bruus · J. P. Kutter
MIC, Department of Micro and Nanotechnology,
Technical University of Denmark,
2800 Kongens Lyngby, Denmark
e-mail: mes@mic.dtu.dk

C. H. Westergaard
Risø-DTU, Vestas Wind Systems A/S,
Frederiksborgvej 399,
4000 Roskilde, Denmark

C. H. Westergaard
Force Technology, Hjørttekærvej 99,
2800 Lyngby, Denmark

Compared to a standard PIV laser system, a LED system has several advantages: small size, adaptability to different fluorescent dyes (a range of wavelengths are available), incoherent light (no speckle or interference phenomena), freely adjustable pulse length and repetition rate, low energy consumption and very low cost. The main disadvantages are the lower light intensity, the broad wavelength spectrum and a broad spatial radiation pattern. Some of these problems can be dealt with by adjustments in the setup, as will be described in more detail below. With the ongoing developments in camera sensitivity as well as LED power, micro-PIV with LED illumination is poised to become a very promising and strong alternative to conventional laser-based systems. As a LED light source provides full freedom in terms of setting pulse lengths and repetition rates, our configuration is not limited to a specific type of application or camera, and it can also be used for other tasks where stroboscopic illumination in microscopy is required (Sinton 2004).

2 Illumination configurations and contrasting method

When applying LED illumination for micro-PIV analysis, both the illumination configuration and the contrasting method need to be chosen according to the optical and material properties of the sample under investigation. In this context, contrast is denoted as the ability to distinguish seeding particles from the background. By use of epifluorescent microscopy, with a barrier filter used to remove excitation light, emitted light from fluorescent particles on a dark background can be recorded. Realizations for micro-PIV using pulsed lasers, CW lasers and white light illumination are common. Obviously, these light sources are quite different in performance, and the excitation light source needs to be chosen in accordance with the requirements of the application. However, with respect to the measured signal the type of light source is relatively unimportant, since it is only used to excite the fluorescent dye embedded in the particles. If fluorescence is not used, contrast can be achieved by either strong scattering of light from particles on dark background, or by weak scattering of light from particles on a bright background of light coming from the backside, either directly or by reflection.

In this paper, we will demonstrate LED illumination applied for recordings of both fluorescent and scattered light, and moreover, supply a comparison between the two.

2.1 Principal configurations

In Fig. 1 the four principal micro-PIV illumination configurations studied in this work are presented: (a) front-lit

configuration, (b) back-lit configuration and (c) and (d) two side-lit configurations. To get a better understanding of the illumination constraints specific to micro-PIV, these configurations should be compared with the description of illumination variants for the miniature PIV system, as supplied by Chételat and Kim (2002).

Optical access is often limited when working with microfluidics. Fluidic connections, reservoirs and auxiliary equipments can clutter the workspace around the sample or chip. In all configurations 1b–d the positioning of the LEDs further limits this workspace. It is, therefore, preferable to work in front-lit mode, where the light from the illumination source is guided through the microscope, and it is in fact the most common choice in micro-PIV when a laser is used. In Fig. 1a such a configuration with a LED is presented. The light from the LED is reflected by the mirror in the filter cube of the microscope and is then focused by the objective onto the sample volume. This method, with LED illumination presented for the first time here, will be referred to as *front-lit configuration* and will be explained in more detail in Subject. 2.2.

In Fig. 1b a back-lit configuration, as presented by Bitsch et al. (2005), is shown. In their system, a single high power LED (Lumileds Luxeon Star, 1W) was used, placed behind a frosted glass plate to diffuse the light, in close proximity to the backside of the sample. Clearly, this configuration has a limitation in that it can only be used for transparent samples. The usability is further limited by the fact that the illuminator needs to be realigned if the sample, or the illuminator, is moved. However, with simple

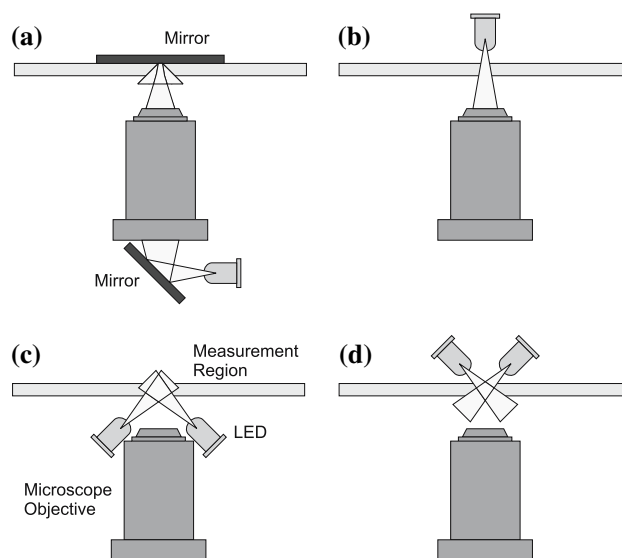


Fig. 1 a Front-lit illumination with a reflector behind the substrate. Note that the figure shows a simplification of the positions of the mirror and the LED. b Back-lit illumination. c Side illumination from objective side. d Side illumination from backside of substrate

adaptations this setup can be improved, as will be explained in Subsect. 2.3.

In micro-PIV, it is generally physically not possible to apply side illumination perpendicular to the viewing angle of the microscope objective. Instead, side illumination will either be applied from the backside or the front side of the sample as shown in Fig. 1c, d, respectively. A system as shown in Fig. 1c, with a ring of 24 LEDs, has been demonstrated by Singh et al. (2001), and is also utilized in the LabSmith SVM340 video microscope (LabSmith 2007). One drawback with this method is that the light distribution to the investigation volume decreases drastically for higher magnification objectives with shorter working distances, as the diodes then need to be placed at a small angle with respect to the object plane. Another drawback is that in order to achieve an even illumination with side illumination, several diodes, which need to be aligned around the objective, are required. For low magnification, long working distance objectives, and for special applications, side-illumination can still be advantageous, but in this study it is not investigated further.

2.2 Novel front-lit configuration

In the front-lit configuration the LED is coupled to the microscope using the optical pathway of a standard epi-fluorescent microscope. In this way, a more rigid system is obtained, as the light source does not need to be realigned every time the substrate under investigation is moved or the microscope objective is exchanged. Moreover, the workspace around the sample or chip is not further limited in this configuration.

The light from a LED is not collimated, but is spreading at a relatively large angle, and consequently the luminous flux diminishes rapidly with increasing distance from the light source (Lumileds 2007). This causes a problem in the front-lit configuration, where the LED needs to be placed relatively far away from the microfluidic system. Moreover, the radiation pattern is typically Lambertian, with a very strong central intensity.

If a LED is placed directly behind the rear lamp house port of an epi-fluorescent microscope, the LED will only illuminate a limited part of the field of view. In order to achieve a more uniform light distribution, expander optics are required, and in this study we have used a fiber adapter. With this solution a larger fraction of the light can be utilized, but if the LED is not aligned accurately, the setup will still produce a curved light intensity distribution over the field of investigation. For the experiments in this study the LED was mounted on a *xyz* optical stage, which allowed the LED to be fine-positioned while light intensity and distribution were observed by the camera. One way to

achieve a flat illumination distribution is by putting a diffuser into the beam path. However, this causes an overall decrease of the illumination intensity over the entire field, and is therefore not recommended.

In the front-lit configuration, you can readily switch between recording fluorescent and scattered light, by exchanging the microscope filter cube. The two filter cubes used in this study are described in Fig. 2. It should be noted that the illumination intensity with the bright field filter cube inserted is not the same as when the I3 filter cube is inserted. This is due to the fact that in the first case, the mirror in the filter cube is a 50–50 beam splitter (half of the light is transmitted and half is reflected), whereas in the second case the mirror is dichroic (reflection or transmission depending on wavelength of incident light).

In the case of scattered light measurements, the most important factor that determines the contrast between the seeding particles and the background is the light reflecting properties of the substrate. This is true both in the situation with extinction of light (background will be even brighter with a more reflective substrate), and in the situation with scattering of light (backward scatter is much weaker than forward scatter). For transparent samples, when the front-lit configuration is preferred over the back-lit configuration, a mirror placed behind the chip can be used as a reflector. This has been shown to be a practical approach (see Sect. 4). With an upright microscope this can be readily achieved by affixing a mirror to the optical stage of the microscope. If the substrate is a naturally non-transparent reflector, such as silicon, the bottom of the microfluidic device itself functions as a mirror. However, if a flow close

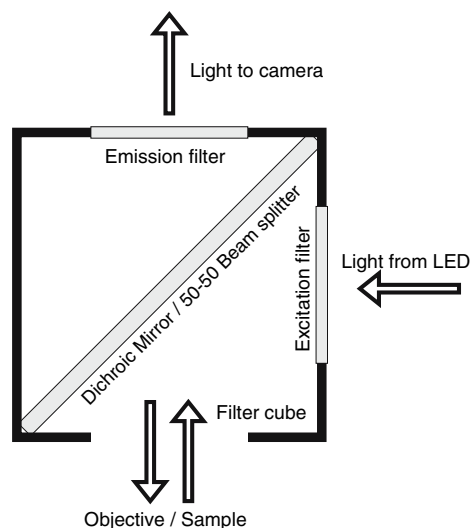


Fig. 2 A sketch of a microscope filter cube. The I3 filter cube has a band pass excitation filter, 450–490 nm, a dichroic mirror, 510 nm, and a long pass emission filter, 515 nm. The bright field, BF, filter cube has no excitation or emission filter, and it has a 50–50 beam splitter instead of a dichroic mirror

to a reflecting boundary is to be inspected, it should be remembered that the images of reflected particles can contribute to the correlation.

In the case of fluorescent light measurements, the fluorescent signal depends on the level of light exposure of the particles. Moreover, the type of fluorescent dye and the amount of dye per particle is of major importance in determining the achievable contrast. Micro-PIV in fluorescent mode is a standard method, and it has been described in numerous publications (e.g., Santiago et al. 1998).

2.3 Improved back-lit configuration

The drawbacks of the back-lit configuration as used in previous studies (Bitsch et al. 2005) are that transparent samples are required, and that the illumination source needs to be placed close to the backside of the microfluidic device. This requirement limits the workspace around the chip, because fluidic connections, reservoirs, and other equipment clutter the region in which the LED needs to be placed. The way the chip is cramped in between the microscope objective and the light source also makes the setup vulnerable, and if the chip is moved, or replaced, it is likely that the alignment of the light source needs to be re-adjusted. Regarding the first requirement, i.e., a transparent sample, this can obviously not be relaxed. However, with the use of optics it is possible to get around the problem with the proximity of the light source. In this study, a low-cost plastic lens, specially designed for Luxeon diodes, was chosen. With such a lens, which focuses the light, the diode can be moved much further away from the chip, while still achieving a high light intensity and a relatively flat intensity profile over the whole illuminated region. In comparison with the close proximity setup, this setup can therefore be used in a larger number of applications, is easier to align and much less sensitive to disturbances.

Additionally, if recordings of fluorescent light are to be made, an excitation filter needs to be fitted between the LED and the sample. This was not attempted in this study; here, the back-lit configuration was only used for recordings of scattered light.

3 Materials and methods

3.1 Experimental setup

Images were recorded with a HiSense MkII progressive scan interline CCD camera (Dantec Dynamics), mounted with a 0.63× TV-adaptor on an epi-fluorescent microscope (Leica DMLB). Objectives used were: N Plan 10×, N Plan

L 20× and PL Fluotar L 63× with numerical apertures (NA) of 0.25, 0.40 and 0.70, respectively. In the front-lit configuration, a blue LED (Lumileds Luxeon K2) was aligned with a xyz optical stage to a fiber adapter with expander optics mounted on the rear lamp port of the microscope. The filter cubes inserted into the optical path were bright field, BF, and I3 (Leica) for recordings in scattered mode and fluorescent mode, respectively (see Fig. 2). In the improved back-lit configuration, on the other hand, the LED was placed below the substrate, and a plastic focusing lens (Carclo-Optics, 20 mm fiber coupling optic) was used.

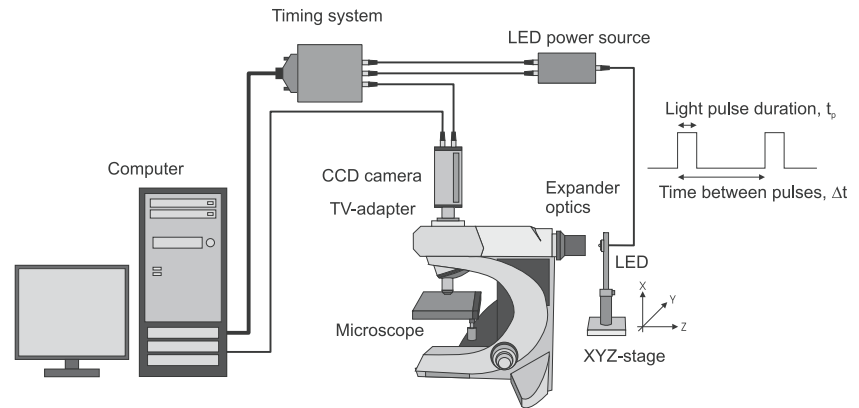
The LED was powered by an in-house built power supply and controlled by a PIV timing system (Dantec Dynamics). If the diode is set to emit light for very short pulse durations, a much higher power than what would be possible for continuous illumination can be used. In the experiments described in this paper, a power supply designed to deliver a power of 26.4 W over the diode was used.

Image acquisition was performed on a PC with Flow-manager software (Dantec Dynamics). A small planar mirror was used for some of the measurements in the front-lit configuration. For reference, green fluorescent polystyrene particles (1 μm diameter, Duke Scientific) were used in all experiments, even though the fluorescent signal was not distinguishable when the bright field filter cube was inserted. For the contrast measurements, particles adhering to the coverslips of glass slides were used, similar to what was described by Meinhart et al. (2000a). For the micro-PIV comparison the flow around a 50 μm squared pillar in a 400 μm wide and 200 μm deep microfluidic channel, fabricated in silicon via deep reactive ion etching (DRIE), was measured. Anodic bonding was used to seal the structure with a 500 μm thick pyrex glass lid on the channel side. A sketch of the whole system with the LED mounted for front-lit illumination, can be seen in Fig. 3.

3.2 Optical power and contrast

The different ways in which contrast between the particles and the background can be enhanced, were described in Sect. 2. Independent of the method used, the contrast, or image quantization (i.e., bits/pixel), is dependant on the level of illumination. As shown by Willert (1996), the image quantization has only a minor influence on the measurement uncertainty in PIV, and an increase from 4 to 8 bits/pixel has hardly any influence on the measurement accuracy. This result is intriguing when comparing LEDs with lasers, because the former delivers considerably less light during short pulse lengths (t_p). If time averaging is used, even lower quantization levels are sufficient (Meinhart et al. 2000b). On the other hand, for super-

Fig. 3 The micro-PIV setup used in the experiments. The LED is positioned as used in the front-lit configuration. Light pulses are synchronized individually with the camera. The camera is running in PIV mode, separating images into image pairs



resolution PIV and particle tracking velocimetry (PTV), larger contrast is beneficial (Keane et al. 1995).

It should be noted that the usable power can differ immensely between different batches of diodes, and even within diodes from the same batch. This has been shown by Benavides and Webb (2005), who have characterized Luxeon diodes. In this study, the primary interest was to compare the illumination properties between different substrates and configurations, and not between different diodes. Therefore, the same diode was used for all measurements presented in this article. The rise time for Luxeon diodes is less than 100 ns, so a pulse length down to 1 μs , which was the shortest one used in this study, is feasible (Lumileds 2007). This has previously been shown by other groups (Estevadeordal and Goss 2005; Benavides and Webb 2005).

Even when the diode is properly aligned and is given sufficient power, the limitations for using LED illumination still depend to a large extent on the properties of the sample under investigation, the particle density, the properties of the tracer particles, the recording system/camera, the applied recording technique, and the requirements on measurement accuracy. Therefore, highly specific limitations for LED illumination in micro-PIV cannot be given. However, if applied correctly, LED illumination can

undoubtedly represent an alternative to other illumination sources for many applications, as evidenced by the results presented below. A guiding comparison between different light sources (calculated for a thin reflecting device under idealized conditions), can be found in Table 1. The numbers are given for a highly sensitive CCD camera, with a pixel size of $7 \times 7 \mu\text{m}^2$. Maximum velocities are calculated for a maximum particle displacement of 1 pixel during exposure, avoiding motion blur.

4 Results

In Fig. 4, normalized spectral light distributions measured below the microscope objective and behind the camera adapter are shown. By comparing spectra (a) and (b) it is seen that the I3 filter cube excitation filter effectively blocks the light from the diode above 500 nm, and thus the camera will only record a fluorescent signal.

The fluorescent particles used in this study have their peak emission wavelength at 508 nm, with a Stokes shift of 40 nm, which is a typical value for fluorescent particles. Nonetheless, a large portion of the emitted light is lost in the I3 filter cube, which is seen by subtracting spectrum (b) from spectrum (c) and comparing the result with spectrum

Table 1 Comparison between different light sources, where “Min t_p ” is the pulse length limitation of the light source, and “Light exposure required” is the minimum exposure time required by the camera (HiSense MkII)

Light source	Min t_p	Light exposure required	$V_{\text{max}10\times}$	$V_{\text{max}63\times}$
Laser, Nd:YAG, flash lamp	~ 10 ns	~ 10 ns	70 m/s	11 m/s
High power LED (scatter)	~ 100 ns	>1 μs	0.7 m/s	0.11 m/s
Normal power LED (scatter)	~ 100 ns	>20 μs	35 $\mu\text{m/s}$	5.6 $\mu\text{m/s}$
Lamp with mechanical shutter	~ 5 ms	<1 ms	140 $\mu\text{m/s}$	22 $\mu\text{m/s}$
Lamp with video camera	25 ms ^a	–	28 $\mu\text{m/s}$	4.4 $\mu\text{m/s}$

V_{max} is calculated for 10 \times and 63 \times magnification using 1 μm particles, and is calculated from the limiting factor of the system (Min t_p or Light exposure required)

^a Video interframe time

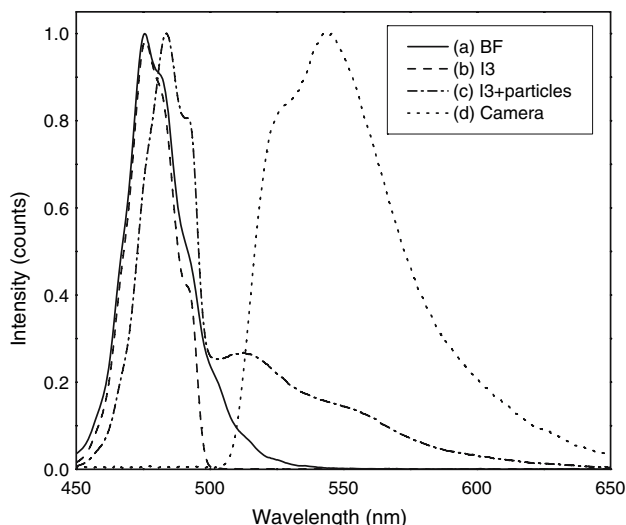
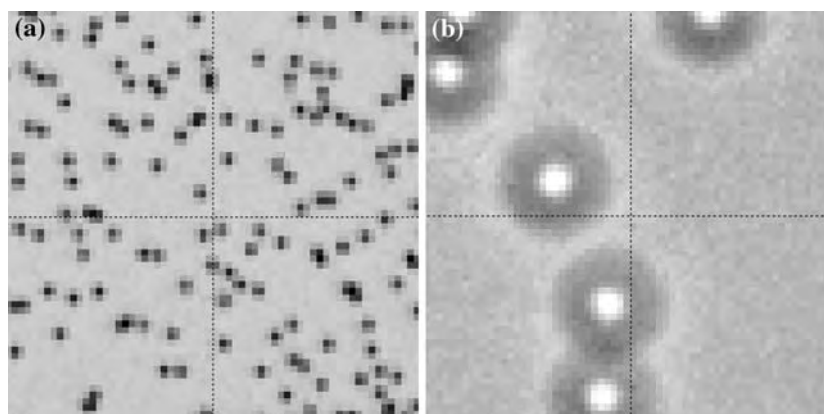


Fig. 4 Normalized spectra of scattered light from a mirror placed below the microscope objective with **a** bright field filter cube inserted, and **b** I3 filter cube inserted. In **c** and **d** a drop containing fluorescent particles is placed underneath the microscope objective. Spectrum **c** is recorded with the spectrometer placed in close proximity to the side of the microscope objective (same as in **a** and **b**), whereas **d** is recorded with the spectrometer placed after the emission filter (in the position of the camera). Since spectra **b** and **d** have no overlap, it can be concluded that spectrum **d** is composed of fluorescent signal only

(**d**). This loss is not an effect from LED illumination in particular, and the same loss is to be expected if a laser is used as excitation source. However, since the optical power is a limiting factor in the case of LED illumination, and typically not so in the case of laser illumination, it would be interesting to explore how much of the emitted light could be collected by using customized filter cubes and particles.

Figure 5 shows two images of particles adhered to the coverslip of a glass slide, recorded with a 10× and a 63× magnification objective, respectively. From a range of such images, while using different objectives (10×, 20× and 63×) and pulse lengths (from 1 to 100 μs with the bright field filter cube, and from 50 μs to 2 ms with the I3 filter

Fig. 5 Images of 1 μm particles adhering to the coverslip of a glass slide recorded with **a** a 10× objective and **b** a 63× objective. For these particular recordings a mirror was used as reflector. The grid is shown for 32 × 32 pixels



cube), quantization levels of particles for each combination were estimated manually. The results from these measurements are shown in Fig. 6. Three different substrates were investigated in the front-lit configuration: cover slips on glass slides with no reflector, cover slips on glass slides placed on a mirror, and cover slips placed directly on a silicon substrate, i.e., a diced silicon wafer. Moreover, the transparent sample was also measured with the three objectives in the improved back-lit configuration. However, in this configuration no fluorescent measurements were attempted.

As can be seen, for the front-lit configuration measurements on scattered light, the contrast (as expressed by the quantization levels, QL) decreases with increasing magnification of the objective (Fig. 6a–c). However, for scattered light measurements the substrate material is the most important factor. With the 10× and the 20× magnification objectives and transparent samples, a 20 times longer pulse length is required to obtain the same contrast as when a mirror is used as back reflector. For the transparent samples without a reflector, a t_p of more than 100 μs was needed with the 63× objective in order to get at least $QL = 4$, and these values are therefore not included in the figure.

Typically, a much longer pulse length is required to obtain the same contrast when fluorescent light is recorded, compared to when scattered light is recorded (Fig. 6, open symbols compared to filled symbols). However, fluorescent measurements are highly dependant on the nature and size of the particles used. As the 63× magnification objective has a significantly shorter focal length than the two other objectives, the thickness of the substrate layer plays a most important role in this case. Therefore, the measurements in Fig. 6c are highly specific for the investigated substrates in this study. It should also be considered that for micro-PIV measurements, the optimal size of the tracer particles, with respect to the measurement uncertainty, depends on the microscope magnification (Raffel et al. 1998). In this study, however, the same 1 μm particles were used in all of the measurements.

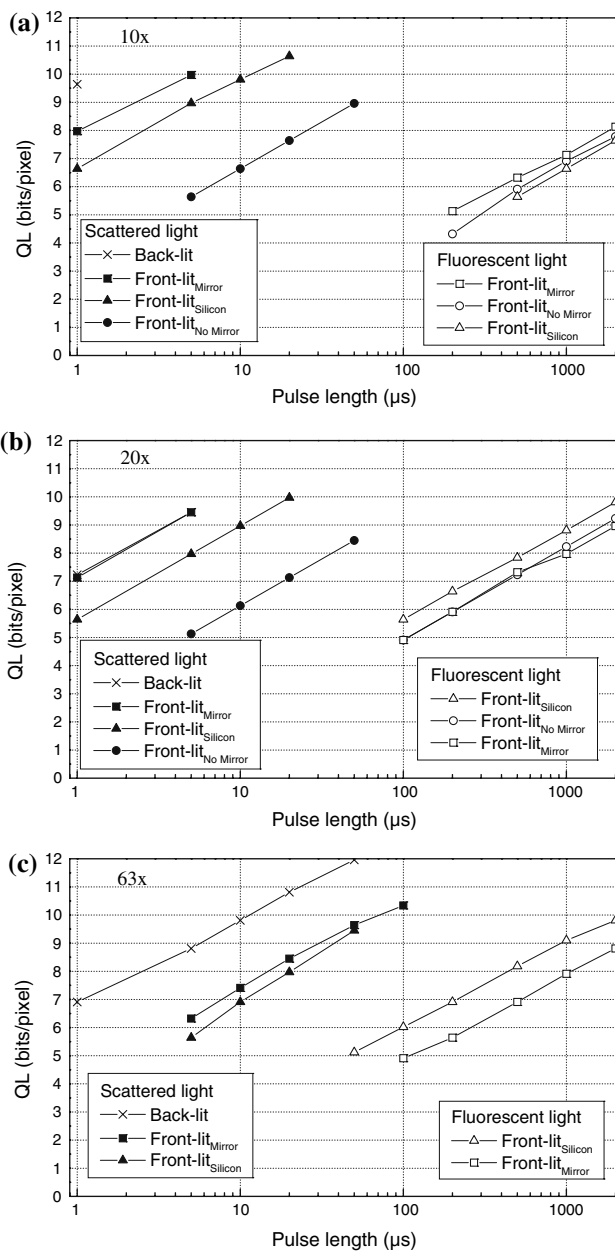


Fig. 6 Quantization levels (QL) for particle images with **a** a 10 \times objective, **b** a 20 \times objective and **c** a 63 \times objective in the front-lit and back-lit configurations. Note that the y-axis increments are not linear but represent a \log_2 scale

In these experiments we used the Dantec HiSense MKII camera with the Sony150ER CCD sensor, having a dynamic range of 1:1800 at a peak quantum efficiency of 70%. In practical PIV terms this camera performs quite similar to the PCO SensiCam QE with the Sony ICX265 CCD having a dynamic range of 1:3000 at a peak quantum efficiency of 62%. These are both about twice as effective as the previous camera generation based on the ICX061 CCDs with a dynamic range of \sim 1:1000 and a quantum efficiency of \sim 50%. Compared to the newer and current

camera generations based on the Kodak KAI series CCDs having a typical dynamic range of \sim 1:1200 and a quantum efficiency of \sim 55%, the newer cameras are approximately 1.5 times less efficient than the one used in this study. Note that the quantum efficiency and dynamic range are sufficient numbers when comparing similar sensors, but one has to be careful not to extrapolate these numbers to other types of cameras/sensors without considering all details of the specifications.

In the last experiment, LED illuminated micro-PIV was used to measure flow velocity around a square pillar, 50 μm on the side, positioned in the middle of a micro-channel, 400 μm wide and 200 μm deep, fabricated in silicon. The flow was driven by a syringe pump (Harvard), with the flow rate set at 0.2 ml/h, and PVC tubes were used as connections to the microdevice. The flow was seeded with 1 μm polystyrene particles, diluted in water to a concentration of 0.25%. In these measurements, the 0.63 \times TV-adaptor and the 63 \times microscope objective were used, providing a field of view of 218 \times 166 μm . The flow of particles was recorded at a depth of \sim 45 μm , both in scattered and fluorescent mode, after background removal providing images as seen in Fig. 7a, b. In each mode, 100 double image frames were recorded with a t_p of 100 μs , and a time between pulses of 1 ms. Vectors were calculated for each double image frame, using the adaptive correlation method (initial interrogation area size: 128 \times 128 pixels), with a final interrogation area size of 64 \times 64 pixels, 50% overlap. The depth of correlation, as given by Olsen and Adrian (2000), was calculated to be \sim 6.0 μm for the fluorescent measurements, and \sim 5.5 μm for the scatter measurements. After removing erroneous velocity vectors through peak validation, the average velocity was calculated for both sets of 100 double image frames (Meinhart et al. 2000b), which resulted in two well matched velocity vector fields, each 31 \times 39 vectors. A comparison between the two modes is seen in Fig. 8, where velocity plots of the u and v velocities for five different cross-sections over the width of the channel are seen. For each cross-section, the average and the maximum difference between the measured velocities in u and v are presented. Considering a bulk flow of \sim 1,000 $\mu\text{m/s}$ the magnitudes of these values indicate the excellent agreement between velocities calculated from, respectively, fluorescent and scattered light measurements. Moreover, it demonstrates the feasibility of both recording techniques, as well as the general applicability of micro-PIV with LED illumination. It is worthy to stress again that a pulse length of 100 μs was chosen to facilitate the comparison between the measurements in scattered and fluorescent mode. High-contrast measurements with much shorter pulse lengths are feasible in the scattered mode (especially with low magnification objectives), thus easily

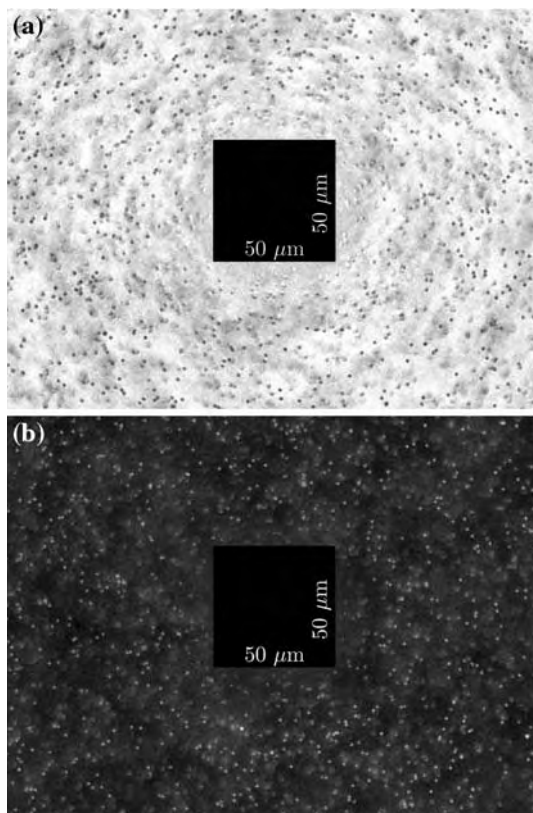


Fig. 7 Background subtracted image frames of $1\ \mu\text{m}$ particles flowing around a $50 \times 50\ \mu\text{m}$ pillar structure at a depth of $45\ \mu\text{m}$. **a** Picture recorded in scattered mode, the bright field filter cube is inserted, and the particles appear *dark* in relation to the background. **b** Picture recorded in fluorescent mode, the I3 filter cube is inserted, and the particles appear *bright* in relation to the background. Both images are recorded with a t_p of $100\ \mu\text{s}$

allowing LED illuminated PIV measurements for other microfluidic systems with flow velocities much higher than those demonstrated here (mm/s–dm/s).

5 Conclusions

In this study, we have shown that light emitting diodes are well suited as illumination sources for micro-PIV measurements. In particular, with the introduction of the *front-lit configuration*, which does not require transparent samples or otherwise imposes limitations to the workspace, the applicability of LEDs has been further improved. Moreover, through improved alignment and the use of higher output powers, we have shown that in scattered mode pulse lengths down to $1\ \mu\text{s}$ are practical, which is more than a factor 10 shorter than what has been shown in previous studies. A comparison between measurements in scattered mode and fluorescent mode was also provided, showing excellent agreement between the two. The main

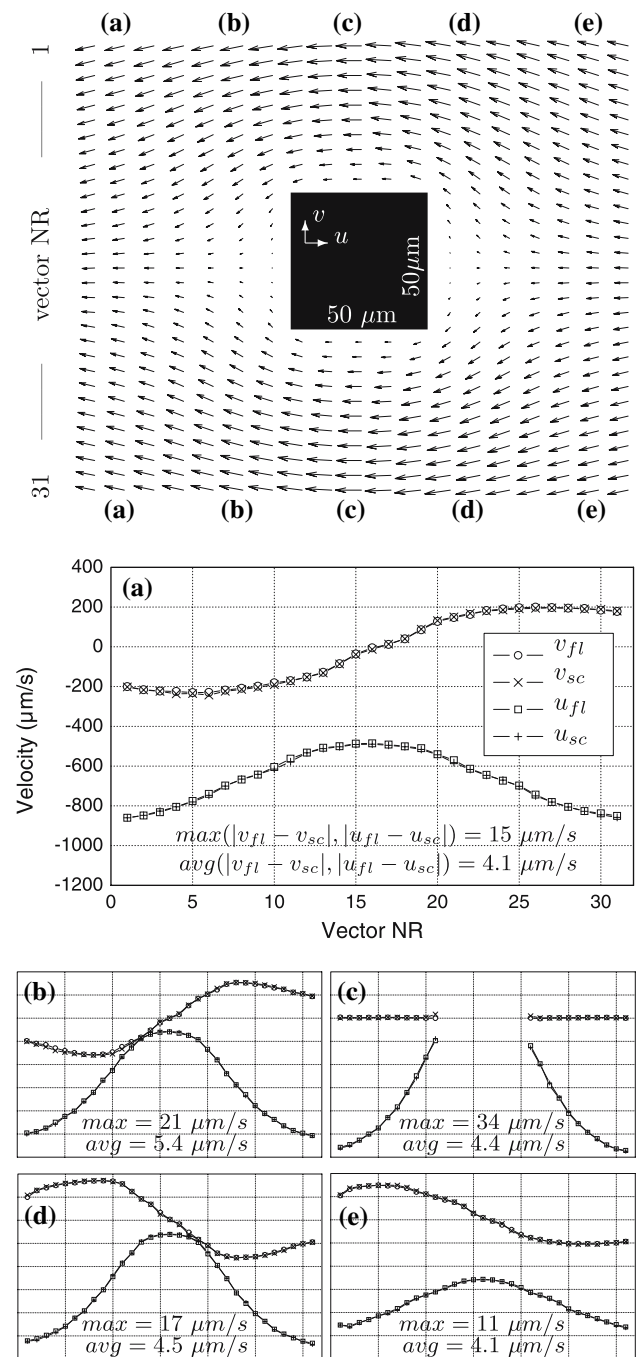


Fig. 8 Top panel shows velocity vector fields around a $50 \times 50\ \mu\text{m}$ pillar recorded in fluorescent mode. For clarity, only every second velocity vector in the channel flow direction is shown. Unit vectors equal $1\ \text{mm/s}$. A comparison between velocity vectors calculated from images recorded in fluorescent *fl* mode and scattered *sc* mode is seen in panels (a–e). The plots are showing the u and v velocities for five different cross sections over the width of the channel. The *scale bars* and *symbols* in panels (b–e) are the same as in panel (a), even though not shown

benefit of the scattered mode over the fluorescent mode when applying LED illumination is that faster flows can be measured.

Due to the large variety in design, materials and fabrication approaches, as well as in the restrictions and demands on the measurements, it is not possible to give a universal answer as to for which micro-PIV measurements a LED can be used or may be advantageous compared to a laser. However, with continuing developments towards increased camera sensitivity as well as towards even brighter LEDs, light emitting diodes have the potential to become even more competitive to other illumination light sources.

Acknowledgments SMH was supported through Copenhagen Graduate School for Nanoscience and Nanotechnology, in a collaboration between Dantec Dynamics A/S and MIC, Technical University of Denmark.

References

- Benavides JM, Webb RH (2005) Optical characterization of ultra-bright LEDs. *Appl Opt* 44(19):4000–4003
- Bitsch L, Olesen LH, Westergaard CH, Bruus H, Klank H, Kutter JP (2005) Micro particle-image velocimetry of bead suspensions and blood flows. *Exp Fluids* 39(3):507–513
- Chételat O, Kim KC (2002) Miniature particle image velocimetry system with LED in-line illumination. *Meas Sci Technol* 13(7):1006–1013
- Estevadeordal J, Goss L (2005) PIV with LED: particle shadow velocimetry (PSV). 43rd AIAA Aerospace Sciences Meeting and Exhibit, Meeting Papers, pp 12355–12364
- Keane R, Adrian R, Zhang Y (1995) Super-resolution particle imaging velocimetry. *Meas Sci Technol* 6(6):754–768
- LabSmith (2007) Svm340 synchronized video microscope. <http://www.labsmith.com/SVM340.html>
- Lumileds (2007) Power Light Source, Luxeon K2 Emitter, Technical Data DS51. <http://www.lumileds.com>
- Meinhart C, Wereley S, Santiago J (2000b) A PIV algorithm for estimating time-averaged velocity fields. *Trans ASME J Fluids Eng* 122(2):285–289
- Meinhart C, Wereley S, Gray M (2000a) Volume illumination for two-dimensional particle image velocimetry. *Meas Sci Technol* 11(6):809–814
- Olsen MG, Adrian RJ (2000) Out-of-focus effects on particle image visibility and correlation in microscopic particle image velocimetry. *Exp Fluids* 29(7):S166–S174
- Raffel M, Willert CE, Kompenhans J (1998) Particle image velocimetry: a practical guide. Springer, Heidelberg
- Santiago JG, Wereley ST, Meinhart CD, Beebe DJ, Adrian RJ (1998) A particle image velocimetry system for microfluidics. *Exp Fluids* 25(4):316–319
- Singh AK, Cummings EB, Throckmorton DJ (2001) Fluorescent liposome flow markers for microscale particle-image velocimetry. *Anal Chem Columbus* 73(5):1057–1061
- Sinton D (2004) Microscale flow visualization. *Microfluidics Nanofluidics* 1(1):2–21
- Willert C (1996) The fully digital evaluation of photographic PIV recordings. *Appl Sci Res* 56(2–3):79–102